IEEE Access
Multidisciplinary | Rapid Review | Open Access Journal

Received February 2, 2021, accepted March 5, 2021, date of publication March 17, 2021, date of current version March 26, 2021.

Digital Object Identifier 10.1109/ACCESS.2021.3066901

Multisector Parabolic Equation Method for Scattering From Impenetrable Objects in Fluid Waveguides

ADITH RAMAMURTI AND DAVID C. CALVO
Acoustics Division, Code 7165, U.S. Naval Research Laboratory, Washington, DC 20375, USA
Corresponding author: Adith Ramamurti (adith.ramamurti@nrl.navy.mil)

This work was supported by the Office of Naval Research (ONR). The work of Adith Ramamurti was supported by NRL's Jerome and Isabella Karle Fellowship Program.

ABSTRACT Parabolic equation methods are a robust and efficient tool for modeling long-range acoustic propagation in range-dependent waveguides. A lesser known, but equally effective, application of parabolic equations is to the scattering problem. In this paper, we study the applicability and accuracy of the multisector parabolic equation approach to scattering from impenetrable objects – first developed approximately two decades ago for convex objects and recently extended to more complex scatterers – in waveguides in two and three dimensions. We benchmark the method in two dimensions in a range-dependent waveguide consisting of two different fluid media and find very good agreement with finite element methods for both forward scattering and backscattering, including the case where the scatterer is located at the interface between the media. Finally, we provide an example of scattering in a large three-dimensional waveguide, which would be extremely computationally intensive using alternate approaches, but is practical using the parabolic equation method.

INDEX TERMS Acoustic parabolic equation, acoustic propagation, acoustic scattering, fluid waveguide, numerical simulation.

I. INTRODUCTION

Parabolic equation (PE) methods are often used to accurately and efficiently model long-range acoustic propagation in complex environments [1]–[3]. While wave propagation has been the primary application of parabolic equation methods in acoustics, a PE technique was developed by Levy and Zaporozhets for modeling scattering from impenetrable objects [4]–[8]. The advantages of this PE-based approach, which we will call the multisector PE method, relative to finite-element methods (FEM), are computational efficiency and ease of implementation [1], [9], [10].

Acoustic target scattering calculations using the Levy-Zaporozhets approach had limitations relating to wide-angle and multiple-scattering phenomena, which restricted the maximum concavity of objects to which the approach could be applied [5], and were limited in their benchmarking. Recent work has established that this method works extremely well for convex scatterers, and can be modified to accurately calculate scattering from a variety impenetrable concave scatterers [10].

The goal of the present work is to interface the multisector PE scattering method with PE-based propagation in two- and three-dimensional fluid waveguides. Three-dimensional scattering from objects in waveguides has historically been computed by solving for the near-field scattering and projecting this to the far-field using approximate Green's functions [11]–[13]. While this works well for layered fluid media, when the waveguide layers are range-dependent in depth and sound speed, these Green's functions become increasingly complicated to compute.

For impenetrable objects, it has been shown that the computational time using the PE to calculate scattering in the near field is approximately the same as FEM approaches in two dimensions, and much faster in three dimensions, with the difference increasing exponentially with the object size [10]. Combining the PE scattering method with PE-based propagation allows for use of the same "back-end" for codes. As such, it does not involve taking propagation results and feeding them into a separate scattering model,

The associate editor coordinating the review of this manuscript and approving it for publication was Gang Mei.

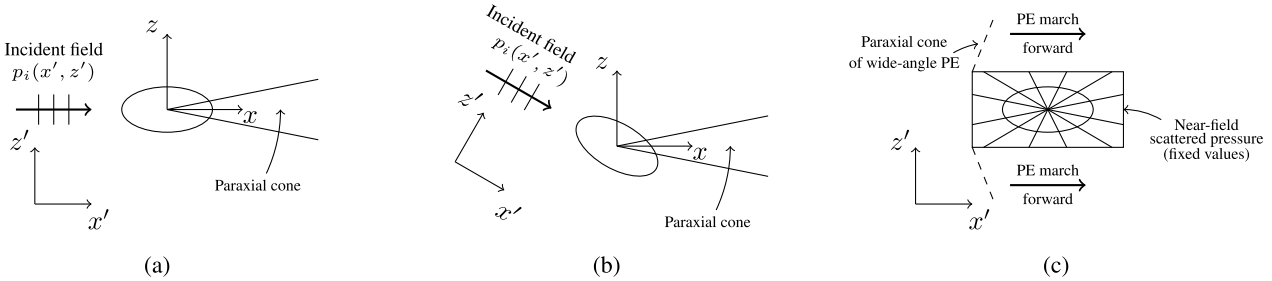

FIGURE 1. Schematic of the parabolic equation scattering method in two dimensions. The "global" waveguide coordinates are denoted $x'z'$, while the "local" scattering coordinates are xz. (a) and (b) show the areas of validity (paraxial cones) of the scattering PE method when marched across the scatterer at two different angles. In (c), the paraxial cones of the different marching angles are stitched together around the scatterer, and are used as input values for the PE, which is used to march the field forward in the waveguide. The PE is then used to march the field backward, using the same input values.

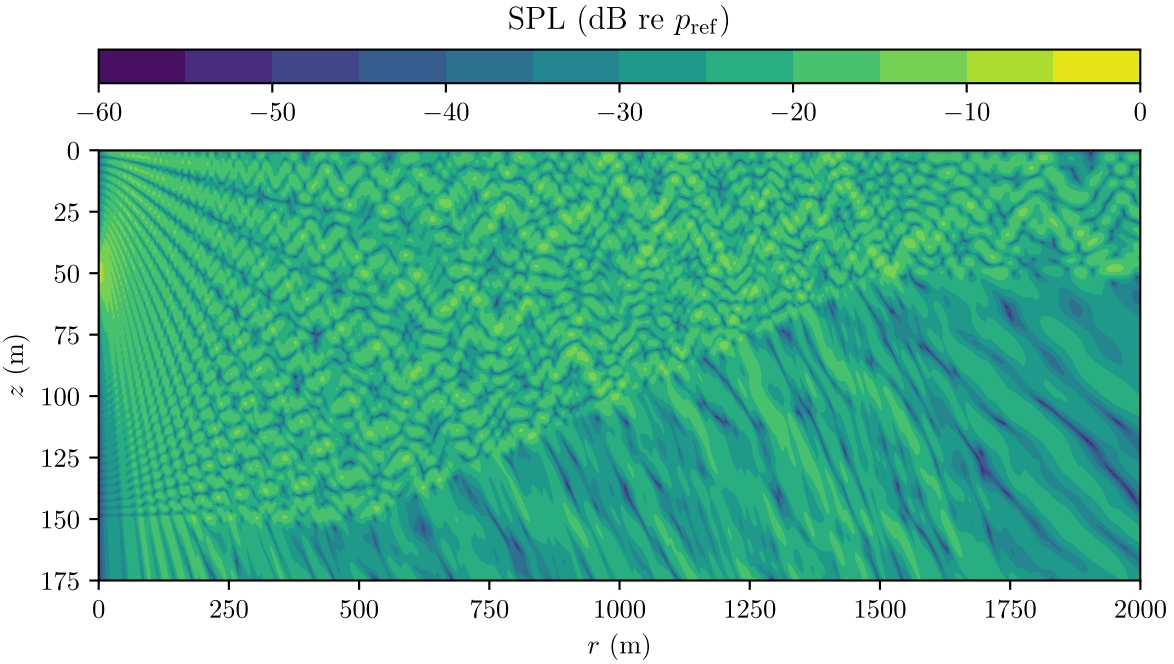

FIGURE 2. Sound pressure level in dB re $p_i(r = 1\text{ m}, z = 50\text{ m})$ for a point source of frequency 250 Hz located at $z_s = 50$ m in the two-fluid waveguide with no scatterer present computed with the parabolic equation.

and then returning the near-field scattering result to a separate propagation model.

In Section II, we will overview the parabolic equation approach to propagation and scattering modeling. To show the robustness of this model, in Sec. III, we will benchmark the results in two-dimensions in a sloping waveguide against a finite-element method approach. Finally, in Sec. IV, we demonstrate the application of this model to scattering in a three-dimensional fluid waveguide with an ocean-like bathymetry.

II. PARABOLIC EQUATION PROPAGATION AND SCATTERING

For clarity, we will briefly overview the aspects of the parabolic equation relevant to this work. The one-way two-dimensional parabolic equation describing acoustic waves propagating in the paraxial direction x is

$$\frac{\partial u}{\partial x} = -ik(1 - Q)u, \tag{1}$$

where $u = pe^{-ikx}$; p is the pressure field;

$$Q = \sqrt{\frac{\rho}{k^2}\frac{\partial}{\partial z}\frac{1}{\rho}\frac{\partial}{\partial z} + \tilde{n}^2} \equiv \sqrt{1 + q};$$

$$q = (\tilde{n}^2 - 1) + \frac{\rho}{k^2}\frac{\partial}{\partial z}\frac{1}{\rho}\frac{\partial}{\partial z},$$

k the reference wave number; ρ the density; and $\tilde{n}(z) = c_0/c_s(1 + i\eta\beta_p)$ the index of refraction, with c_0 the reference speed of sound, c_s the speed of sound, $\eta = 1/(40\pi \log_{10}(e))$,

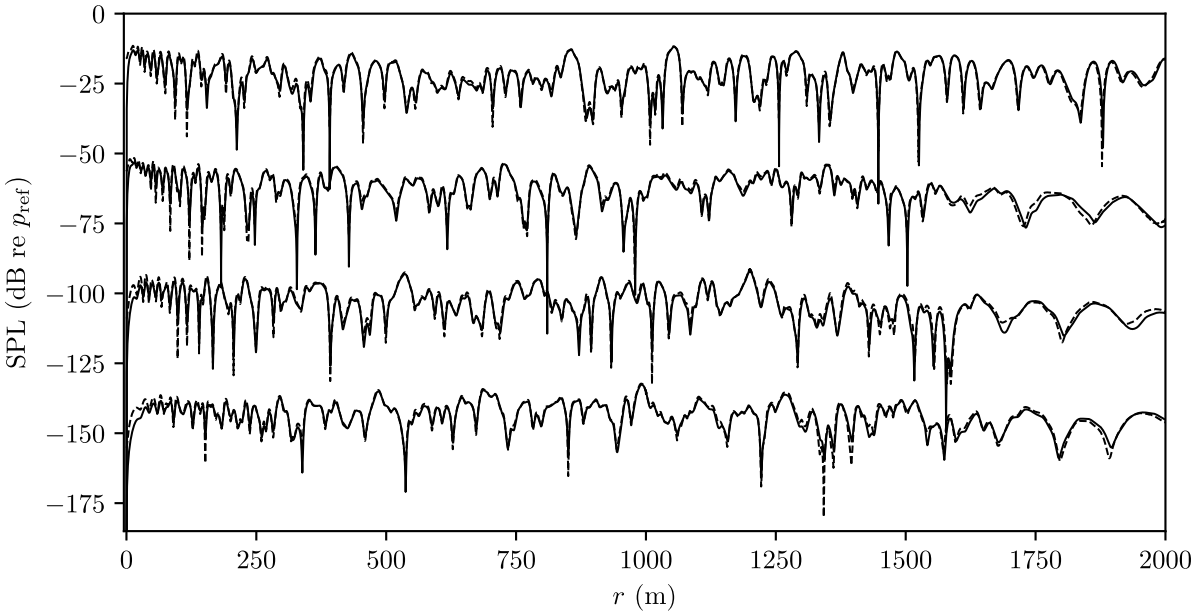

FIGURE 3. Sound pressure level in dB re $p_i(r = 1\text{ m}, z = 50\text{ m})$ along lines of constant depth for a point source of frequency 250 Hz located at $z_s = 50$ m in the two-fluid waveguide with no scatterer present computed with the parabolic equation. The solid lines are the PE computation, and the dashed are from the FEM model. From top to bottom, the depths corresponding to the lines are 40, 60, 80, and 100 m, with offsets of 0, 40, 80, and 120 dB, respectively.

and β_p the attenuation per wavelength in dB. We assume the pressure field has standard exp $-i\omega t$ time dependence.

When modeling propagation, the standard approach is to approximate the square root operator Q with a Padé approximant [14]. The sum form of the Padé approximant is

$$1 - Q = \sum_{n}^{N} \frac{A_{n,N} q}{1 + B_{n,N} q}, \tag{2}$$

while the product form of the operator is

$$Q = \prod_{n}^{N} \frac{1 + C_{n,N} q}{1 + B_{n,N} q}, \tag{3}$$

with coefficients $A_{n,N}$, $B_{n,N}$, $C_{n,N}$ for the Padé expansion of order N. These coefficients are given as

$$\begin{aligned} A_{n,N} &= \frac{a_{n,N} e^{-i\alpha/2}}{(1 + b_{n,N}(e^{-i\alpha} - 1))^2}, \\ B_{n,N} &= \frac{b_{n,N} e^{-i\alpha}}{1 + b_{n,N}(e^{-i\alpha} - 1)}, \\ C_{n,N} &= \frac{c_{n,N}}{1 + b_{n,N}(e^{i\alpha} - 1)}, \end{aligned} \tag{4}$$

with

$$\begin{aligned} a_{n,N} &= \frac{2}{2N+1} \sin^2\left(\frac{n\pi}{2N+1}\right), \\ b_{n,N} &= \cos^2\left(\frac{n\pi}{2N+1}\right), \\ c_{n,N} &= \sin^2\left(\frac{n\pi}{2N+1}\right). \end{aligned} \tag{5}$$

The parameter α is the rotation angle of the approximation in the complex plane, and appropriate choice of angle allows for accurate treatment of evanescent waves ($q < -1$) [15]. As an example of how to implement this in a numerical scheme, we can substitute the sum form into the parabolic equation and discretize in range with steps of size Δx. This yields an iterative formula to propagate the field u from range step $m-1$ to m:

$$\begin{aligned} &(1 + (B_{n,N} - ik\Delta x A_{n,N})q)u^{(n)} \\ &\quad = (1 + (B_{n,N} + ik\Delta x A_{n,N})q)u^{(n-1)}, \\ &\quad n = 1 \ldots N, \end{aligned} \tag{6}$$

where $u^{(0)} = u^{m-1}$ and $u^{(N)} = u^m$ [3]. The finite difference formulas used to implement the operator q can be found in Ref. [16].

To accurately model propagation in range-dependent waveguides, we need to account for the field backscattered from sloping waveguide boundaries. The standard parabolic equation conserves pressure across range steps, and therefore does not account for backscattered pressure, leading to incorrect results. One way to correct for this is to enforce energy conservation between range steps. The approximation of energy conservation, going from region A to region B, is given by

$$(k_A/\rho_A)^{1/2} u_i = (k_B/\rho_B)^{1/2} u_t, \tag{7}$$

where u_i is the incident pressure and u_t is the transmitted pressure [17]. This conservation is applied at each range step *prior* to propagation, and only the transmitted pressure u_t is propagated forward using the parabolic equation.

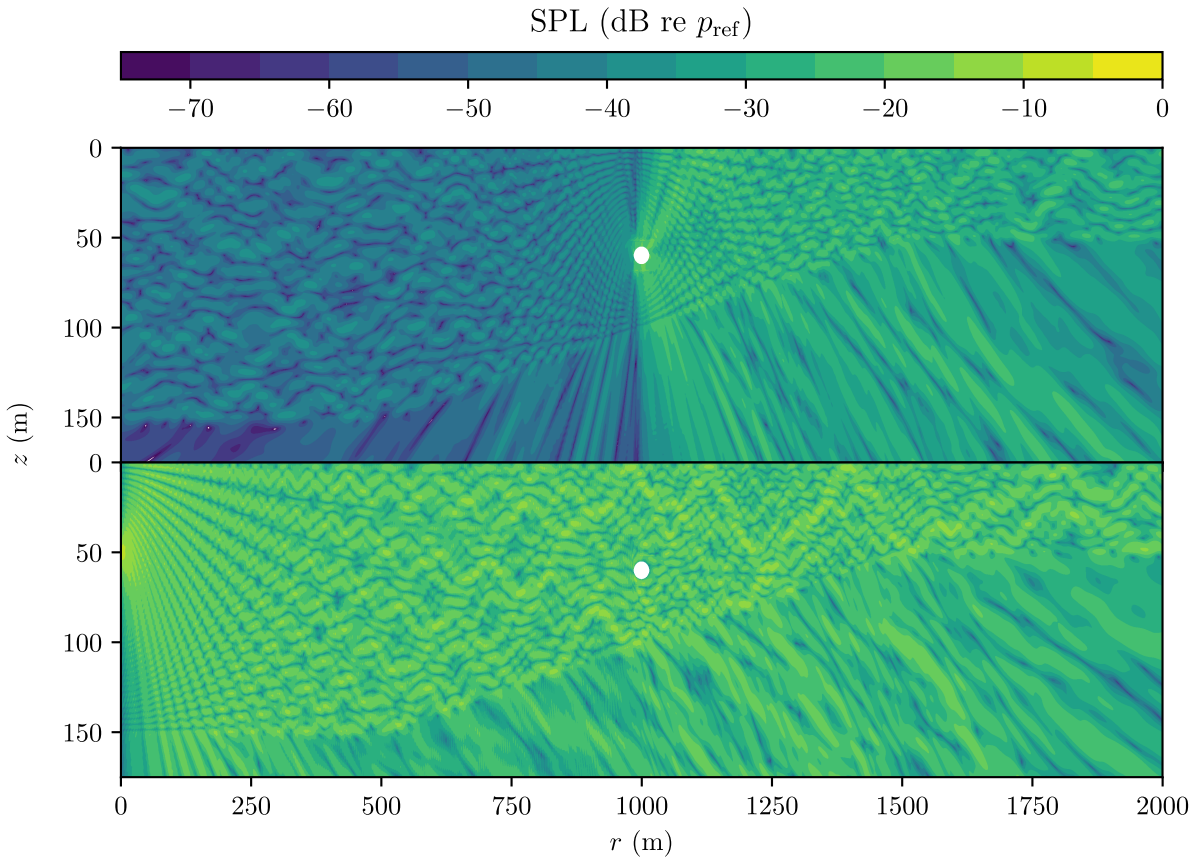

FIGURE 4. Sound pressure levels in dB re $p_i(r = 1\ \mathrm{m}, z = 50\ \mathrm{m})$ for scattering from a soft ellipse with axes $a_r = 15$ m and $a_z = 5$ m in the water column of a fluid-fluid waveguide. The center of the ellipse is located at $(r, z) = (1000\ \mathrm{m}, 60\ \mathrm{m})$. The top panel shows the scattered field from the ellipse, while the bottom panel shows the total field (incident and scattered). Both fields are as computed by the parabolic equation method.

In a domain with a scatterer, a given total field p can be decomposed into its incident p_i and scattered p_s components. The PE-scattering method solves for the scattered field, using the incident field to calculate a source term on the boundary of the impenetrable object. The parabolic equation for the forward-scattered field is identical to that of the total field,

$$\frac{\partial u_{\mathrm{s}}}{\partial x} = -ik(1 - Q)u_{\mathrm{s}}. \tag{8}$$

A general form of the boundary condition on an impenetrable object is

$$\gamma \frac{\partial p}{\partial \vec{n}} + \zeta p = 0, \tag{9}$$

where γ and ζ are free parameters and $\vec{n}$ is the vector normal to the boundary of the object; the parameter cases ($\gamma = 0,\ \zeta = 1$) and ($\gamma = 1,\ \zeta = 0$) correspond to objects with soft (pressure release) and hard (rigid) boundaries, respectively. In terms of the incident and scattered fields, we have

$$\gamma \frac{\partial p_s}{\partial \vec{n}} + \zeta p_s = -\gamma \frac{\partial p_i}{\partial \vec{n}} - \zeta p_i.$$

This boundary condition can be written for the field u_{s},

$$\gamma n_x \left(\frac{\partial u_{\mathrm{s}}}{\partial x} + iku_{\mathrm{s}} \right) + \gamma n_z \frac{\partial u_{\mathrm{s}}}{\partial z} + \zeta u_{\mathrm{s}} = -\gamma e^{-ikx} \frac{\partial p_i}{\partial \vec{n}} - \zeta e^{-ikx} p_i, \tag{10}$$

where n_x, n_z are the components of the normal vector to the object.

Substituting the narrow-angle PE ($Q \approx 1 + q/2$) for the x derivative of (10) yields the boundary condition

$$ik\gamma n_x \left(\frac{(\tilde{n}^2 - 1)}{2} + \frac{\rho}{2k^2} \frac{\partial}{\partial z} \frac{1}{\rho} \frac{\partial}{\partial z} + 1 \right) u_{\mathrm{s}} + \gamma n_z \frac{\partial u_s}{\partial z} + \zeta u_s = -\gamma e^{-ikx} \frac{\partial p_i}{\partial \vec{n}} - \zeta e^{-ikx} p_i, \tag{11}$$

which has no range derivative dependence. All the discussion above is identical in three dimensions, with

$$Q = \sqrt{\frac{\rho}{k^2} \left(\frac{\partial}{\partial y} \frac{1}{\rho} \frac{\partial}{\partial y} + \frac{\partial}{\partial z} \frac{1}{\rho} \frac{\partial}{\partial z} \right) + \tilde{n}^2}.$$

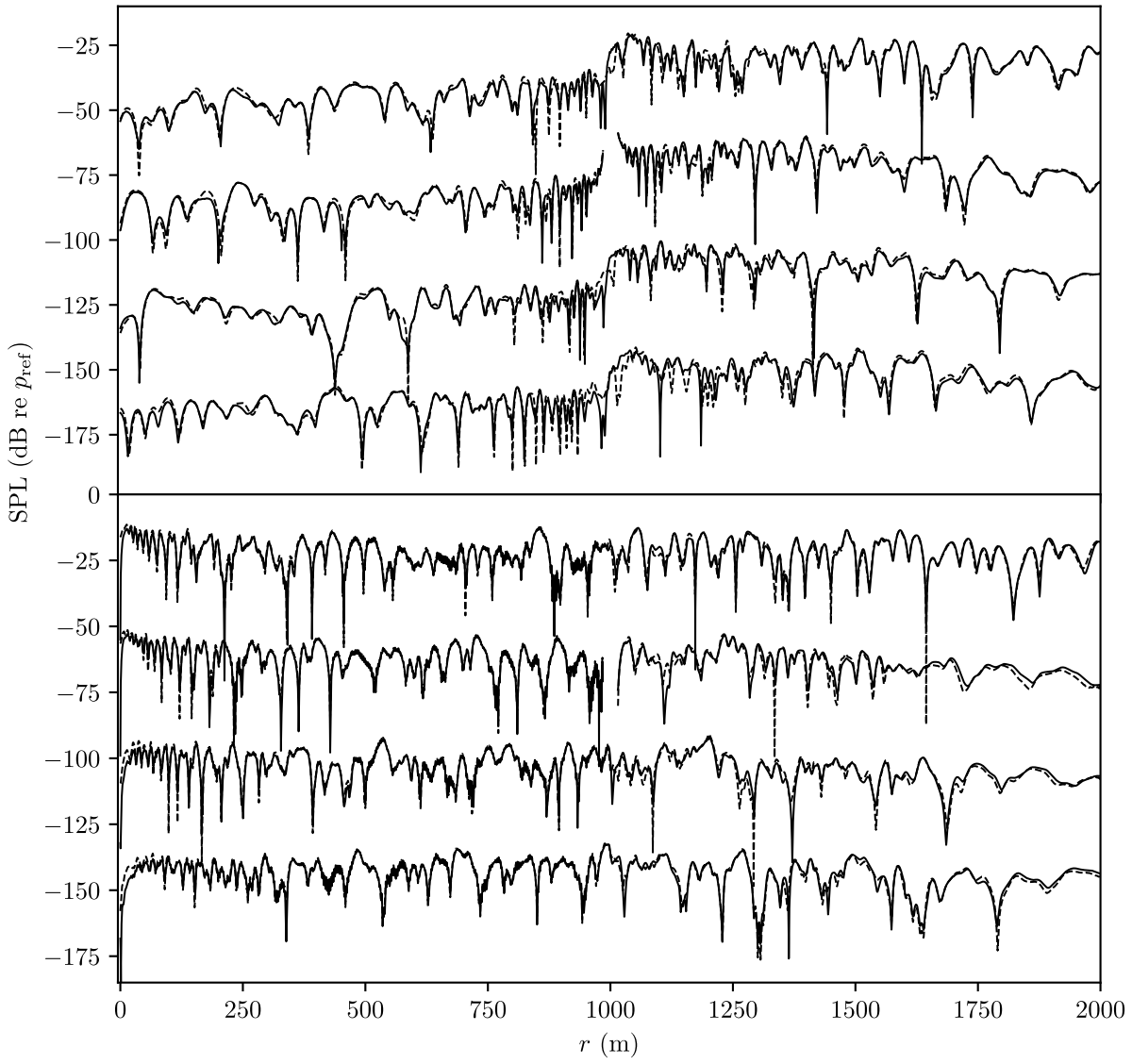

FIGURE 5. Sound pressure level in dB re $p_i(r = 1\text{ m}, z = 50\text{ m})$ along lines of constant depth in a fluid-fluid waveguide for the case of a soft ellipse with axes $a_r = 15$ m and $a_z = 5$ m in the water column. The center of the ellipse is located at $(r, z) = (1000\text{ m}, 60\text{ m})$. The top panel is for the scattered field from the soft ellipse, while the bottom panel is for the total field. The solid lines are the PE computation, and the dashed are from the FEM model. From top to bottom on each panel, the depths corresponding to the lines are 40, 60, 80, and 100 m, with offsets of 0, 40, 80, and 120 dB, respectively.

Numerical solutions using the PE-scattering method are implemented via a finite-difference algorithm on a Cartesian grid in a small domain containing the scatterer. The scatterer is discretized in a stair-step manner, and the field is marched in different paraxial directions relative to the scatterer using the parabolic equation, with the scattered field sourced by the appropriate boundary conditions on the surface of the scatterer. For each direction of marching (denoted by coordinate system xz, relative to the scatterer's coordinate system $x'z'$), the pressure within the paraxial cone – with width determined by the wide-angle form of the PE used – is the only part of the scattered field that is valid. The different paraxial cones are then stitched together to obtain the full near-field scattered pressure around the object, hence the name *multisector*. This near-field pressure is then propagated away from the scatterer using the standard parabolic equation formalism. This process is illustrated in Fig. 1 for a two-dimensional object and forward PE propagation. For further description and examples of the scattering method, see Refs. [9], [10].

We know from previous studies that the scattering method itself can accurately and efficiently model scatterers of various shapes and orientations for free-field target strength calculations. The focus of this work is therefore to see how well the PE scattering method can incorporate an incident waveguide field to produce the near-field scattered pressure about an object; how well that near-field pressure can be

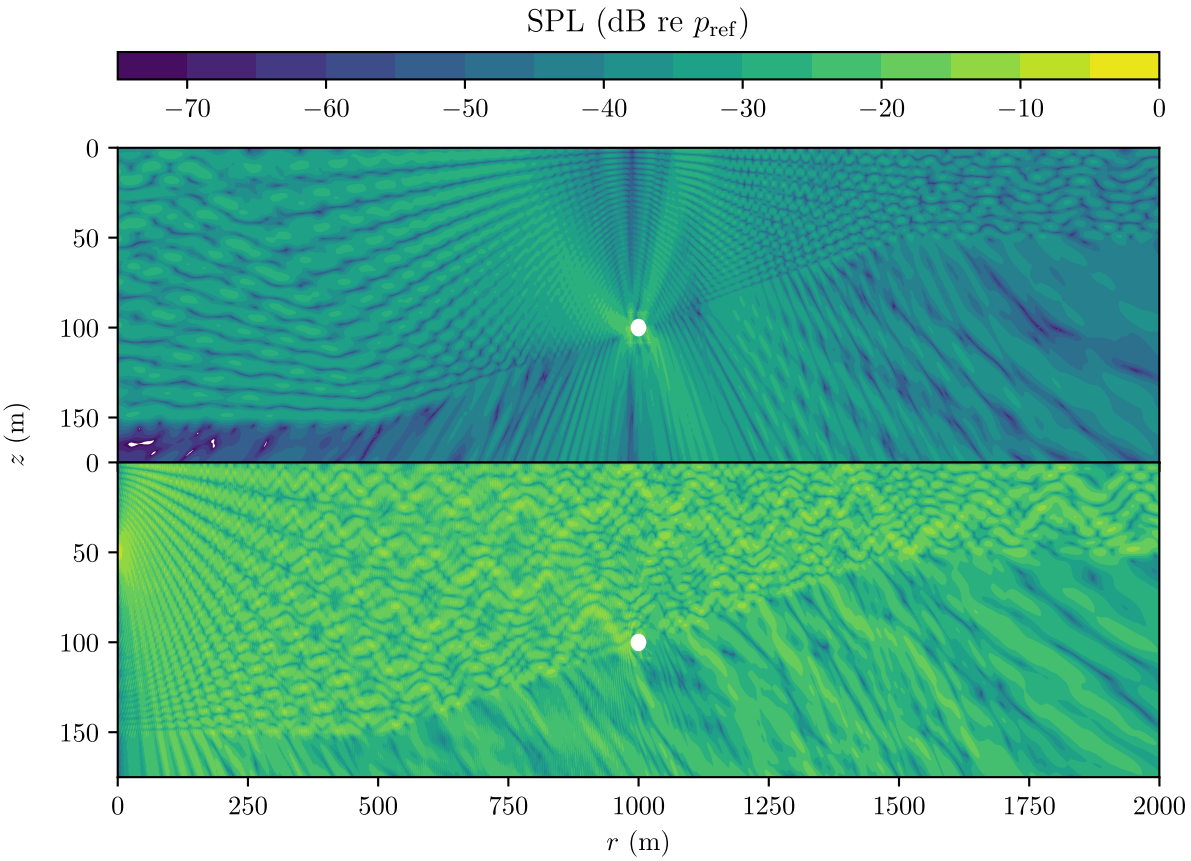

FIGURE 6. Sound pressure levels in dB re $p_i(r = 1\text{ m}, z = 50\text{ m})$ for scattering from a hard ellipse with axes $a_r = 15$ m and $a_z = 5$ m at the interface in a fluid-fluid waveguide. The center of the ellipse is located at $(r, z) = (1000\text{ m}, 100\text{ m})$. The top panel shows the scattered field from the ellipse, while the bottom panel shows the total field (incident and scattered). Both fields are as computed by the parabolic equation method.

used to accurately source a propagation model to the far-field in a range-dependent waveguide; and how well the method handles a changing index of refraction around the scatterer.

III. BENCHMARKING IN TWO DIMENSIONS

We will benchmark the performance of the scattering method in a two-dimensional fluid waveguide consisting of two fluid media with different acoustic properties. These cases are easily modeled by finite-element methods and allow for comparison between the methods in terms of both accuracy and speed; in this work, we will use the COMSOL Multiphysics software [18] to obtain these benchmarks.

We begin by describing the waveguide. The water column has depth 150 m from $r = 0$ m to $r = 500$ m, and then a constant slope upward from 150 m to 50 m depth from $r = 500$ m to $r = 1500$ m, and then constant 50 m depth from $r = 1500$ m to $r = 2000$ m. The top of the waveguide has a pressure release boundary, and below 175 m depth, we implement a perfectly-matched layer to absorb any incident pressure [19]. The water column has constant sound speed $c_p = 1500$ m/s, density $\rho = 1000$ kg/m^3, with no absorption. The "sediment" has $c_p = 1800$ m/s, density $\rho = 2000$ kg/m^3, and attenuation $\beta_p = 0.1$ dB/λ.

All two-dimensional examples have a point source of frequency 250 Hz located at $z_s = 50$, and pressures in this paper are presented in dB, with the reference pressure $p_{\text{ref}} \equiv p_i(r = 1\text{ m}, z = 50\text{ m})$, where p_i is the pressure field in the waveguide with no scatterer present.

For propagation, we use the parabolic equation with 8 Padé terms, and a complex plane rotation angle of $\alpha = \pi/2$ rad. The grid spacings Δr and Δz are both set to $\lambda/10 = 0.6$ m. For the scattering computation Δr was set to 0.3 m. The matrix equations were solved using the Eigen linear algebra package [20] in C++. For the propagation modeling, we used the implementation of the SparseLU solver, while for the scattering computation, we used the BiCGSTAB solver. For the finite element model, the maximum element size is set to $\lambda/6$.

Fig. 2 is a plot of the sound pressure level computed by the PE for this setup. Fig. 3 shows the pressures computed by the PE and FEM models at depths of 40, 60, 80, and 100 m, from top to bottom. The 40 m line is not offset, while the 60, 80, and 100 m lines are offset by 40, 80, and 120 dB, respectively. Overall, we see excellent agreement at all depths between the parabolic equation and finite element approaches, even when the sound propagates into the bottom medium.

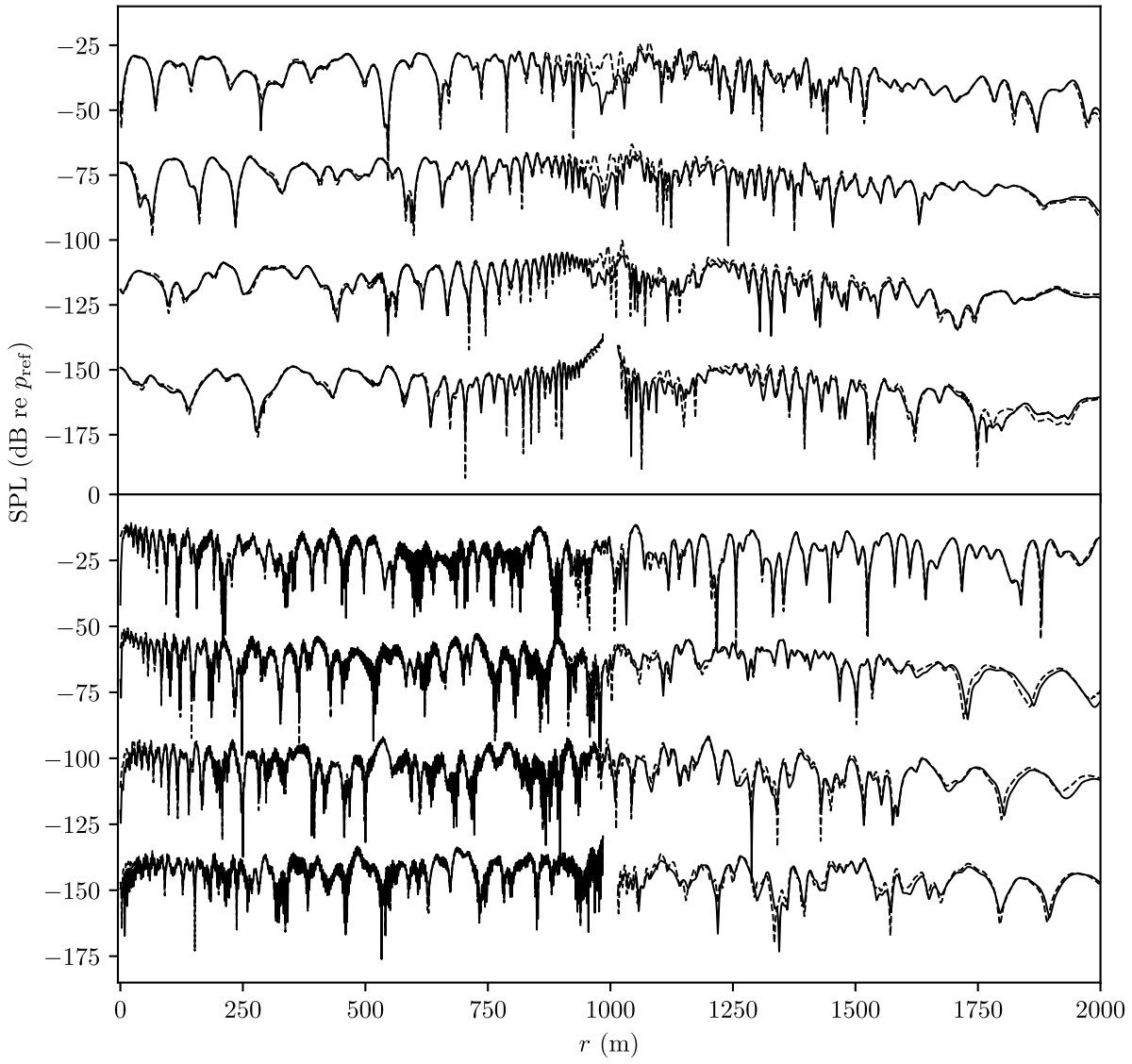

FIGURE 7. Sound pressure level in dB re $p_i(r = 1\text{ m}, z = 50\text{ m})$ along lines of constant depth in a fluid-fluid waveguide for the case of a hard ellipse with axes $a_r = 15$ m and $a_z = 5$ m at the interface between the two media. The center of the ellipse is located at $(r, z) = (1000\text{ m}, 100\text{ m})$. The top panel is for the scattered field from the soft ellipse, while the bottom panel is for the total field. The solid lines are the PE computation, and the dashed are from the FEM model. From top to bottom on each panel, the depths corresponding to the lines are 40, 60, 80, and 100 m, with offsets of 0, 40, 80, and 120 dB, respectively.

With the knowledge that our incident fields are accurate, we will look at two illustrative examples, the first with a soft (pressure release) ellipse in the water column, and the second with a hard (rigid) ellipse at the interface between the two fluid media. In both instances, the center of scatterer will be located at $r = 1000$ m, and have

The first example is for a soft ellipse with axes $a_r = 15$ m, $a_z = 5$ m, located at $r = 1000$ m and $z = 60$ m, in the water column above the sloping interface. Fig. 4 shows contour plots of the scattered field (top panel) and the total field (bottom panel), which is the sum of the scattered field and the background pressure field shown in Fig. 2. Fig. 5 shows the sound pressure level as computed by the PE (solid lines) and FEM (dashed lines) methods at depths of 40, 60, 80, and 100 m, with offsets of 0, 40, 80, and 120 dB, respectively. In general, we see excellent agreement between the two methods in the forward and backward directions. In the backscattering direction, the small oscillations induced in the total field are captured perfectly.

The area of largest difference in the scattered fields between the two approaches is directly above and below the scatterer. This is due to the fact that the PE, even when using many Padé terms, has a paraxial cone that does not include propagation completely perpendicular to the marching direction. We note that this difference is small when looking at the total field. If one, however, is concerned with the field directly

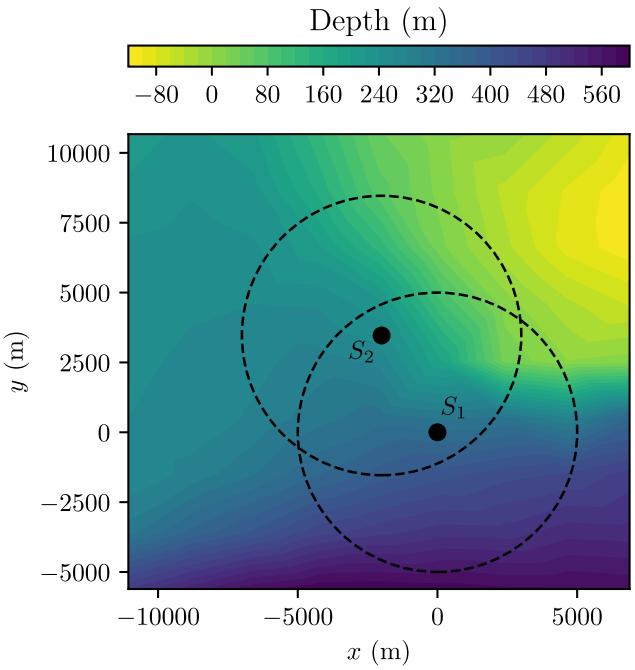

FIGURE 8. The bathymetry used in the example of three-dimensional propagation and scattering. The source is located at point S_1 (the origin), at depth $z = 40$ m. The scatterer is located at point S_2 at depth $z = 180$ m, with coordinates $(r, \theta) = (4000\text{ m}, 2\pi/3)$, corresponding to (x, y) location $(-2000\text{ m}, 3646\text{ m})$. The dashed circles denote the ranges modeled by the parabolic equation for the incident and scattered fields.

above or below the scatterer, it is possible to use the same approach as done here for the forward and backward scattering to march instead in the upward and downward directions, using the same near-field scattered field as a source. In this approach, at the top interface, one could use a two-way PE method to capture perpendicular reflections off the surface from the upward march [21], [22].

The next example we show is for a hard ellipse of the same dimensions, located at $r = 1000$ m and $z = 100$ m depth, straddling the interface of the two media. Fig. 6 shows contour plots of the scattered field from the hard ellipse (top panel) and the total field (bottom panel), and Fig. 7 shows the sound pressure level as computed by the PE (solid lines) and FEM (dashed lines) methods at depths of 40, 60, 80, and 100 m, with offsets of 0, 40, 80, and 120 dB, respectively. Once again, we see excellent agreement between the two approaches, except for the region directly above the scatterer. In this case, the rapid oscillations of the backscattered total field are larger than that of the previous case, but are still captured perfectly.

For these examples, using a laptop with a six-core (twelve openMP threads) Intel i9 2.9 GHz processor, the COMSOL solutions took 65 seconds and 71 seconds for each case (not including meshing time), respectively, while the PE method took 28 and 32 seconds for each case, respectively. Even for simple two-dimensional examples, the PE approach gives excellent results with great efficiency as compared to other approaches. The PE is significantly faster at the propagation

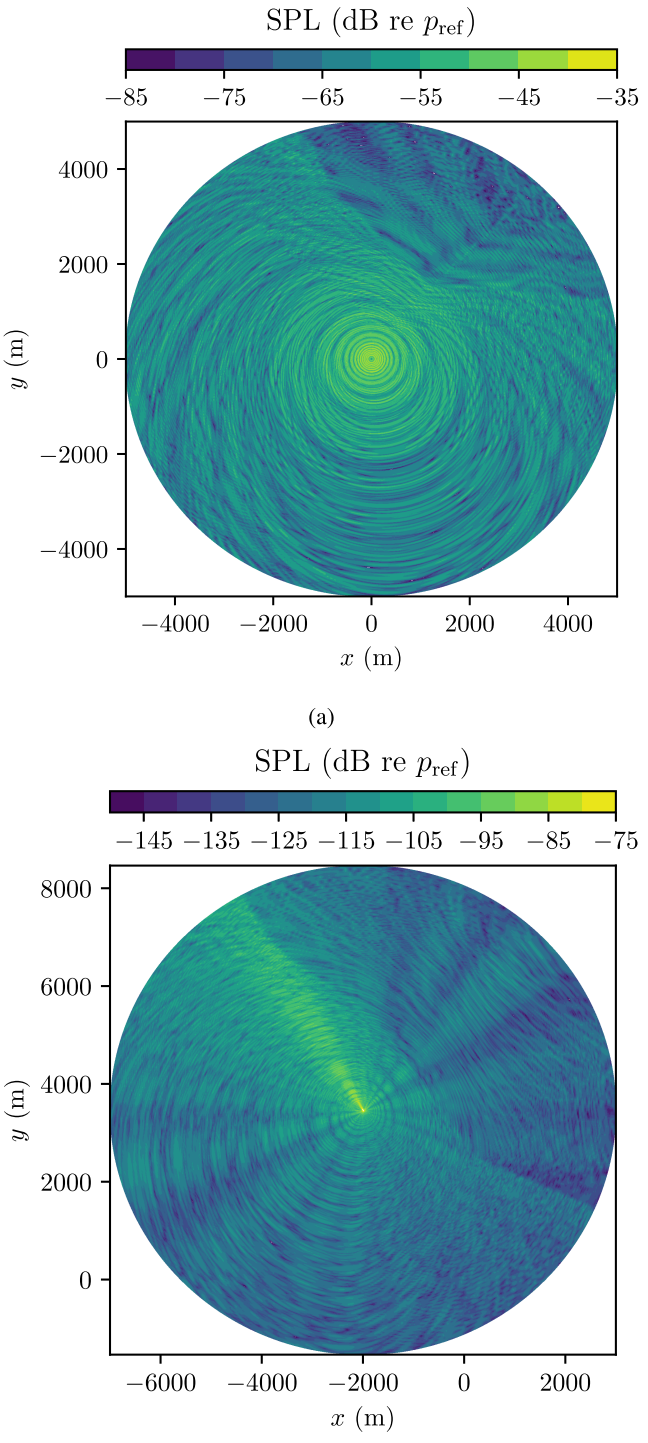

FIGURE 9. (a) Sound pressure level in the example three-dimensional waveguide at $z = 180$ m depth for a point source of frequency 250 Hz located at $z = 40$ m depth with no scatterer present. (b) Sound pressure level at $z = 180$ m depth of the scattered field from an ellipsoid of dimensions $a_r = 25$ m, $a_\perp = 10$ m located at $(r, \theta) = (4000\text{ m}, 2\pi/3)$ in the example three-dimensional waveguide.

portion of the problem, and the scattering takes comparable time between the two approaches in two dimensions, depending on the size of the object [10].

IV. THREE-DIMENSIONAL EXAMPLE

In three dimensions is where the PE approach comes into its own. Computing long range acoustic propagation in realistic environments is extremely computationally intensive using FEM approaches, and these calculations generally cannot be carried out on a desktop computer. On the other hand, modeling three dimensional propagation with the parabolic equation is efficient and accurate [1], [3]. When computing scattering from impenetrable objects, it has been shown that, for most three-dimensional cases, the PE method is more efficient than the FEM, as well [10].

For illustrative purposes, we will now provide an example of the PE method being used to compute long-range scattering in a three-dimensional fluid waveguide with an ocean-like bathymetry. The bathymetry used for this model is shown in Fig. 8. The source, at the location marked S_1 (the origin), is point source with frequency 250 Hz and depth 40 m. The scatterer is a soft ellipsoid with axes $a_r = 25$ m, $a_\perp = 10$ m, at the location marked S_2, with coordinates $(r, \theta, z) = (4000\text{ m}, 2\pi/3, 180\text{ m})$. The ranges modeled for the initial propagation and the scattered field are denoted by the dashed circles of radius 5 km around each location.

The propagation computation for the incident field was carried out in cylindrical coordinates with five Padé terms in the z and θ directions, with grid spacing 0.6 m in the r and z directions and 1/1440° in the θ direction. The matrix equation was solved using an alternating direction-implicit scheme, as implemented in Ref. [3]. The local scattering computation had grid spacing 0.6 m in the y and z directions, and 0.3 m in the x direction, and the outward propagation of the scattered field was computed using the same parameters as the propagation of the incident field.

Fig. 9a shows the pressure field without the scatterer present at depth 180 m. Fig. 9b shows the subsequent scattered field propagating outward from the scatterer at depth 180 m. The pressures are presented in dB with reference pressure $p_{\text{ref}} \equiv p_i(r = 1\text{ m}, z = 40\text{ m})$.

In terms of computational time, the entire modeling process (initial propagation, scattering calculation, and propagation of the scattered field) took 38.5 CPU hours, of which 1.6 CPU hours (4.1%) were for the scattering computation. One should note that the solver back end for both portions is identical, and thus any computational speedup in solving the matrices in the propagation portion of the code directly translates to the scattering computation, and therefore the proportion will remain approximately the same.

V. SUMMARY

Parabolic equation approaches have long yielded efficient computational models for long-range propagation of pressure fields in waveguides. In this work, we have shown that the previously established techniques for computing acoustic scattering from impenetrable objects using the multisector parabolic equation can be interfaced with propagation models to yield accurate far-field scattered pressures in fluid waveguides. In two dimensions, we benchmarked the results against finite-element methods, and found excellent agreement between the two approaches. We then provided an example of computing propagation and scattering in three-dimensions, which, using the parabolic equation method, is practical to carry out on a standard desktop computer. In a fluid-elastic waveguide, which would be more representative of an ocean with a solid bottom, this method works identically for impenetrable acoustic scatterers in the water column. For penetrable or elastic scatterers, or scatterers embedded in a solid medium, further study is necessary.

ACKNOWLEDGMENT

The authors thank M. D. Collins and J. F. Lingevitch for useful discussions.

REFERENCES

[1] F. B. Jensen, W. A. Kuperman, M. B. Porter, and H. Schmidt, *Computational Ocean Acoustics*. New York, NY, USA: Springer, 2000, doi: 10.1007/978-1-4419-8678-8.

[2] M. D. Collins, "Foreword to the special issue," *Wave Motion*, vol. 31, pp. 97–99, Feb. 2000, doi: 10.1016/S0165-2125(99)00037-2.

[3] F. Sturm, "Numerical study of broadband sound pulse propagation in three-dimensional oceanic waveguides," *J. Acoust. Soc. Amer.*, vol. 117, no. 3, pp. 1058–1079, Mar. 2005, doi: 10.1121/1.1855791.

[4] A. A. Zaporozhets and M. F. Levy, "Modelling of radiowave propagation in urban environment with parabolic equation method," *Electron. Lett.*, vol. 32, no. 17, pp. 1615–1616, 1996, doi: 10.1049/el:19961060.

[5] M. F. Levy and A. A. Zaporozhets, "Target scattering calculations with the parabolic equation method," *J. Acoust. Soc. Amer.*, vol. 103, no. 2, pp. 735–741, Feb. 1998, doi: 10.1121/1.421198.

[6] A. A. Zaporozhets, "Application of vector parabolic equation method to urban radiowave propagation problems," *IEE Proc.-Microw., Antennas Propag.*, vol. 146, no. 4, p. 253, 1999, doi: 10.1049/ip-map:19990567.

[7] A. A. Zaporozhets and M. F. Levy, "Bistatic RCS calculations with the vector parabolic equation method," *IEEE Trans. Antennas Propag.*, vol. 47, no. 11, pp. 1688–1696, Nov. 1999, doi: 10.1109/8.814948.

[8] M. Levy and A. Zaporozhets, "Parabolic equation techniques for scattering," *Wave Motion*, vol. 31, pp. 147–156, Feb. 2000, doi: 10.1016/S0165-2125(99)00042-6.

[9] M. Levy, *Parabolic Equation Methods for Electromagnetic Wave Propagation* (IEE Electromagnetic Waves Series), vol. 45. Edison, NJ, USA: IET, 2000, doi: 10.1049/PBEW045E.

[10] A. Ramamurti and D. C. Calvo, "Multisector parabolic-equation approach to compute acoustic scattering by noncanonically shaped impenetrable objects," *Phys. Rev. E, Stat. Phys. Plasmas Fluids Relat. Interdiscip. Top.*, vol. 100, no. 6, Dec. 2019, Art. no. 063309, doi: 10.1103/PhysRevE.100.063309.

[11] M. D. Collins and M. F. Werby, "A parabolic equation model for scattering in the ocean," *J. Acoust. Soc. Amer.*, vol. 85, no. 5, pp. 1895–1902, May 1989, doi: 10.1121/1.397896.

[12] M. Zampolli, A. Tesei, G. Canepa, and O. A. Godin, "Computing the far field scattered or radiated by objects inside layered fluid media using approximate Green's functions," *J. Acoust. Soc. Amer.*, vol. 123, no. 6, pp. 4051–4058, Jun. 2008, doi: 10.1121/1.2902139.

[13] A. Sarkissian, B. Houston, J. Bucaro, and L. Kraus, "Near-field to far-field projection algorithm for free-field or buried scatterer," *J. Acoust. Soc. Amer.*, vol. 133, no. 2, pp. 912–917, Feb. 2013, doi: 10.1121/1.4773860.

[14] M. D. Collins, "Higher-order Padé approximations for accurate and stable elastic parabolic equations with application to interface wave propagation," *J. Acoust. Soc. Amer.*, vol. 89, no. 3, pp. 1050–1057, Mar. 1991, doi: 10.1121/1.400646.

[15] F. A. Milinazzo, C. A. Zala, and G. H. Brooke, "Rational square-root approximations for parabolic equation algorithms," *J. Acoust. Soc. Amer.*, vol. 101, no. 2, pp. 760–766, Feb. 1997, doi: 10.1121/1.418038.

[16] M. D. Collins and W. L. Siegmann, *Parabolic Wave Equations With Applications*. New York, NY, USA: Springer, 2019, doi: 10.1007/978-1-4939-9934-7.

[17] M. D. Collins and E. K. Westwood, "A higher-order energy-conserving parabolic equqation for range-dependent ocean depth, sound speed, and density," *J. Acoust. Soc. Amer.*, vol. 89, no. 3, pp. 1068–1075, Mar. 1991, doi: 10.1121/1.400526.

[18] COMSOL AB, Stockholm, Sweden. *COMSOL Multiphysics V. 5.4*. Accessed: Mar. 18, 2021. [Online]. Available: https://www.comsol.com

[19] J. P. Berenger, "A perfectly matched layer for the absorption of electromagnetic waves," *J. Comput. Phys.*, vol. 114, pp. 185–200, Oct. 1994.

[20] G. Guennebaud and B. Jacob. (2010). *Eigen V3*. [Online]. Available: http://eigen.tuxfamily.org

[21] M. D. Collins and R. B. Evans, "A two-way parabolic equation for acoustic backscattering in the ocean," *J. Acoust. Soc. Amer.*, vol. 91, no. 3, pp. 1357–1368, Mar. 1992, doi: 10.1121/1.402465.

[22] J. F. Lingevitch, M. D. Collins, M. J. Mills, and R. B. Evans, "A two-way parabolic equation that accounts for multiple scattering," *J. Acoust. Soc. Amer.*, vol. 112, no. 2, pp. 476–480, Aug. 2002, doi: 10.1121/1.1490364.

ADITH RAMAMURTI received the A.B. degree in mathematical physics and music from Brown University, Providence, RI, in 2013, and the Ph.D. degree in physics from Stony Brook University, Stony Brook, NY, in 2018.

While at Stony Brook University, his research focused on studying non-perturbative phenomena of quantum chromodynamics in heavy-ion collisions. He is currently a Research Scientist with the U.S. Naval Research Laboratory, Washington, DC, USA, where his research focuses on numerical methods for underwater scattering and propagation.

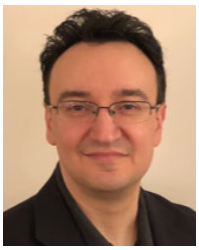

DAVID C. CALVO received the B.S. degree in mechanical engineering from Carnegie Mellon University, Pittsburgh, PA, in 1995, and the M.S. and Ph.D. degrees in mechanical engineering from the Massachusetts Institute of Technology, Cambridge, MA, in 1997 and 2001, respectively.

He is currently the Head of the Advanced Acoustic Systems Development Section with the Acoustics Division, U.S. Naval Research Laboratory, Washington, DC, USA. His research interests include underwater acoustic propagation and scattering, acoustic sensing, sound isolation and production, acoustic metamaterials, numerical methods, marine electromagnetics, and nonlinear dispersive wave theory.